Alkali-activation of metakaolin and blast furnace Portland cement blends

Alcali-ativação de blendas de cimento Portland de alto-forno e metacaulim

DOI:10.34117/bjdv6n12-792

Recebimento dos originais: 10/12/2020
Aceitação para publicação: 06/01/2021

Cláudio Mesquita Campinho de Azevedo
Mestrando em Engenharia Civil pela UFF
Graduado em Arquitetura e Urbanismo pela UGF
Programa de Pós-Graduação em Engenharia Civil – Universidade Federal Fluminense – UFF
Endereço: Rua Passo da Pátria, 156, São Domingos, Niterói
claudio.mesquita@gmail.com

Cléo Márcio de Araújo Santana
Mestrando em Engenharia Civil pela UFF
Graduado em Engenharia Mecânica pela UFPA
Programa de Pós-Graduação em Engenharia Civil – Universidade Federal Fluminense – UFF
Endereço: Rua Passo da Pátria, 156, São Domingos, Niterói
cmarcios@gmail.com

Eliane Fernandes Côrtes Pires
Doutora em Engenharia Civil pela UFF
Graduada em Engenharia Mecânica pela UFJF
Laboratório de Estruturas e Argamassa – Escola de Engenharia da Universidade Federal Fluminense – UFF. Endereço: Rua Passo da Pátria, 156, São Domingos, Niterói
elianepires01@hotmail.com

Paulo Feliciano Soares Filho
Doutor em Engenharia Mecânica pela UFF
Graduado em Engenharia Mecânica pelo CEFET-RJ
Laboratório de Ensaios Destrutivos – Instituto Federal do Rio de Janeiro – IFRJ/Campus Paracambi
Endereço: Rua Sebastião Lacerda, S/N, Centro, Paracambi, RJ
paulo.filho@ifrj.edu.br

Elie Chahdan Mounzer
Doutor em Ciência dos Materiais pelo IME
Graduado em Engenharia Civil pela UVA
Laboratório de Estruturas e Argamassa – Escola de Engenharia da Universidade Federal Fluminense – UFF. Endereço: Rua Passo da Pátria, 156, São Domingos, Niterói
emounzer@yahoo.com.br

Felipe José da Silva
Doutor em Ciência dos Materiais pelo IME
Graduado em Engenharia Mecânica pela FTESM
Laboratório de Ensaios Não-Destrutivos – Instituto Federal do Rio de Janeiro – IFRJ/Campus Paracambi
Endereço: Rua Sebastião Lacerda, S/N, Centro, Paracambi, RJ, CEP 26600-000
felipe.silva@ifrj.edu.br

ABSTRACT
The addition of certain pozzolanic materials to Portland cement significantly changes the properties of the hardened matrix. If it has too high content of blast furnace slag, as the case of blast furnace Portland cements (BFPC), the early and late compressive strengths can be severely delayed or reduced. The objective this work was to investigate the potential of alkali-activation of BFPC and metakaolin (MK) blends by different types and contents of alkali-activators. The results clearly showed the influence of the MK pozzolanic activity and the type and content of activator used, in the development of compressive strengths of BFPC-MK blends. Microstructural analysis by SEM/EDS, DSC and XRD shown that the consumption of portlandite and the extra formation of C-S-(A)-H phases are the main positive effects registered. However, MK also promotes the formation of ettringite and unstable hydrated calcium aluminate phases, which, with the course of hydration, undergo a change in structure and volume loss, contributing to the reduction of final strengths. Content of 25% MK and 7.5% Na_2SiO_3 provided the best mechanical strength. The microstructures formed showed greater formation of ettringite, however there was also a reduction in portlandite and massive formation of C-S-H and C-S-(A)-H products.

Keywords: Alkali-activation, Metakaolin, Portland cement, Blast furnace slag.

RESUMO
A adição de certos materiais pozolânicos ao cimento Portland altera significativamente as propriedades da matriz endurecida. Se ele tiver um teor muito alto de escória de alto-forno, como ocorre nos cimentos Portland de alto-forno (BFPC), as resistências à compressão inicial e final podem ser severamente retardadas ou reduzidas. O objetivo deste trabalho foi investigar o potencial de ativação alcalina de blendas de BFPC e metacaulim (MK) por diferentes tipos e conteúdos de ativadores alcalinos. Os resultados mostraram claramente a influência da atividade pozolânica do MK e do tipo e conteúdo do ativador utilizado, no desenvolvimento das resistências à compressão das blendas BFPC-MK. As análises microestruturais por MEV/EDS, DSC e DRX mostraram que o consumo de portlandita e a formação extra das fases C-S-(A)-H são os principais efeitos positivos registrados. Porém, o MK também promove a formação de fases etringita e aluminato de cálcio hidratado instável, que, com o decorrer da hidratação, sofre alteração na estrutura e perda de volume, contribuindo para a redução das resistências finais. Teores de 25% MK e 7,5% Na_2SiO_3 proporcionaram a melhor resistência mecânica. As microestruturas formadas apresentaram maior formação de etringita, porém também houve redução da portlandita e formação massiva dos produtos C-S-H e C-S-(A)-H.

Palavras-chave: Álcali-ativação, Metacaulim, Cimento Portland, Escória de alto-forno.

1 INTRODUCTION

Pozzolanic materials have been the most widely used technological choice worldwide to improve the properties of Portland cement mortars and concretes. Characteristics such as resistance to acids and sulphates, low heat release during hydration and low permeability are the main reported benefits [1, 2]. However, increasing the content of pozzolans, decreases the rate of strength development, a fact that makes pozzolanic cements little applicable in situations where high initial strengths are necessary [3, 4]. As they are relatively inert in the presence of water, when incorporated into cement, pozzolans depend on the release of calcium ions during hydration to begin to react. Pozzolanic reactions consume calcium ions, reducing the formation of calcium hydroxides [5]. When they are rich in silica, they generate C-S-H phases with a high Si/Ca ratio, which contributes to maintaining a lower pH than the Portland cement matrix without addition, and therefore more stable in aggressive environments [6]. Alkali-activation of granulated blast furnace slag is a technology used for almost a century. In 1925, Odler [4] realized that alkaline sulfates present in water in contact with these slags promoted the hardening reaction. In the 1940s, researchers concluded that alkalis were responsible for awakening the latent properties of slag, for promoting pH levels capable of solubilizing the vitrified compounds present in granulated slag, promoting the formation of hydrated phases of high mechanical strength and stability in highly aggressive environments to Portland cement [7, 8]. However, alkalis in this case causes the dissolution of gehlenite ($Ca_2Al_7SiO_7$) by removing aluminum and the subsequent formation of hydrated aluminates and silicates [9].

The free alkalis in the contact solution, tend to crystallize after hydration of the alkali-activated Portland cement. However, in contact with the amorphous or poorly crystallized silica of the pozzolan and with the help of OH^- ions, they promote the formation of stable silica compounds with high mechanical strengths.

There are still many works on the use of this technology to activate pozzolanic reactions. Some researchers criticize the use of alkali activation only for blast furnace slag and use the alkali-silica reaction (silica fume and NaOH) to produce high quality composites by activation in the fresh state [10]. However, they warn that these systems cannot be cured in water, due to the solubility of the formed alkaline silicates.

In this work, an orthogonal factorial arrangement was used to explore the effect of alkali-activation of blast furnace Portland cement and metakaolin blends, from four different sources of alkali. The microstructure formed, and some physical and mechanical properties developed at various ages were evaluated and compared.

2 MATERIALS AND METHODS

Materials used include blast furnace Portland cement - CPIII-32 (BFPC), provided by LafargeHolcim-Brasil, Brazil. It has about 50% of granulated blast furnace slag addition, according to the manufacturer's data, and meets the requirements of NBR 16697:2018 standard. Metakaolin (MK) was obtained by calcining kaolin in a muffle furnace at 700 ºC for 6 h. Kaolin was supplied by Brasilminas S.A. and comes from deposits located in the State of Rio Grande do Norte, Brazil. Fine aggregate used was Brazilian standard sand (NBR 7215:2019), obtained from Technological Research Institute (IPT) located in São Paulo State, Brazil. The sand was dried at 105 ºC for 24 h before used.

To carry out the study of alkali-activation, different sources of alkali were adopted: Na_2O, from

NaOH; K_2O, from KOH and K_2CO_3, all "pro-analysis", manufactured by VETEC S.A., and Na_2SiO_3, from alkaline sodium silicate (SS) with Na_2O/SiO_2 weight ratio = 0.49, manufactured by Gessy-Lever S.A. Table 1 shows the chemical composition and some physical properties of the materials used.

Table 1. Chemical composition and physical properties of the materials used.

Material	SiO_2	Al_2O_3	CaO	K_2O	Na_2O	MgO	Fe_2O_3	SO_3	IR[a]	LOI[b]	SG[c]	SA[d]
BFPC	28.2	6.7	53.0	0.3	0.1	3.6	1.0	3.2	1.0	1.7	2.96	210.85
MK	44.4	39.8	0.01	0.33	0.04	0.01	0.3	-	47.9	14.4	2.56	1665.17
SS	35.6	-	-	-	17.3	-	-	-	36.9	44.3	1.37	-

a - Insoluble residue in hydrochloric acid (NBR NM 15:2012).
b - Loss on ignition by calcination at 950 ± 50 ºC (NBR NM 18:2012).
c - Determination of specific gravity by the "Le Chatelier bottle" (NBR 16605:2017) (kg/m^3).
d - Specific area by nitrogen absorption – BET (m^2/kg).

The alkali source reagents were dissolved in distilled water to obtain the alkali-activating solution in the required molarity and water/binder ratio. The solution was stored at room temperature for 24 hours before use. The content of MK varied from 0 to 50% and alkali, from 0 to 15%, by weight, in relation to the sum of the MK weight and the granulated blast furnace slag weight present in the BFPC.

To prepare the paste samples, MK and BFPC, were dry mixed for 5 min to obtain a homogenous mixture. The homogenized mixture was poured into the mixer over the previously inserted alkaline solution for 30 seconds, turned on at low speed (rotation around axis at 140 ± 5 rpm and planetary movement at 62 ± 5 rpm). Then, was increased to high speed (rotation around axis at 285 ± 10 rpm and planetary movement at 125 ± 10 rpm) and maintained for 60 seconds. Immediately after mixing, the paste was collected with a spatula and inserted into the mold of the Vicat apparatus for testing the initial and finish setting times, according to NBR NM 65:2002. Mortars were prepared according to NBR 7215:2019, using the four fractions of standard sand. These procedures were carried out in an air-conditioned environment, with a temperature between 18 and 22 ºC. The water/binder ratio was kept constant and equal to 0.48 for mortars and 0.35 for pastes. The mortars compressive strength at 4 hours, and 1, 3, 7, 28 and 90 days of ages was determined according to the NBR 7215:2019. Except for the age of 4 hours, all mortars were demolded after 24 hours and cured in the air at 25 ± 2 ºC and at 70 ± 10% relative humidity until the date of the tests.

Microstructural analyzes were performed on raw materials and paste samples for identification and semi-quantification of the formed phases. The crystallographic characterization by X-ray diffraction (XRD) was carried in a SIEMENS diffractometer model D5000. The copper tube had Kα λ=1,54 Å and was operated at 40 kV with a 110 mA current. Thermal analyzes were performed in a SHIMADZU, model DCS-50. The samples were heated from room temperature to 700 ºC, at a rate of 20 ºC per minute in an argon atmosphere. The scanning electron microscopy (SEM) with secondary electronic images was performed in a JEOL low vacuum scanning electron microscope, model JSM 5800-LV, equipped with a dispersive energy spectrometer (EDS- NORAN), with ZAF and Bence-Albee method for compositional correction. The primary electron beam was generated from a tungsten filament whose voltage varied between 10 and 25 kV. The working distance was fixed between 20 and 35 mm.

In order to minimize the number of experiments without increasing the variance of the distribution of the correlation results between the variables, an orthogonal "half-factorial" arrangement (Plackett-

Burman design) with 3 independent variables was established: X1, X2, X3 in 2 normalized levels (-1, +1) and with 2 replicates in the center. The orthogonal and "half-factorial" or minimal factorial arrangement has the following advantages [11, 12]: Reduces the number of experiments; Allows trend analysis; Maintain parameters independently; The replica in the center allows the maintenance of the orthogonality of the system while revealing the experimental error; Enables the development of linear models with variance compatible with the experimental error; It allows to obtain inflection points from the mathematical model.

The study variables were: X1 = BFPC content (50 <X1 <100%), that is, 0 to 50% MK; X2 = Alkali content (0 <X2 <15%); X3 = Alkali source (Na_2O, K_2O, Na_2SiO_3 and K_2CO_3).

The number of Symmetric Levels (l) was 2, the number of Variables (NX) was 3, the number of replicates (NR) was 2 and the number of Experiments (NE) was equal to:

$$l^{NX} + NR = 2^3 + 2 = 10 \quad (1)$$

However, a minimal factorial design, based on the Plackett-Burman plans, was adopted, as shown in Table 2 and Figure 1.

The design of experiments is considered an orthogonal arrangement if the covariance matrix is diagonal (parameters not correlated), which is obtained if ΣXi = 0 in the normalized variable [11].

Table 2. Minimum number of experiments (orthogonal "half-factorial" design).

	X_1	X_2	X_3
	-1	-1	+1
	+1	+1	+1
	+1	-1	-1
Replicas in the center =>	-1	+1	-1
	0	0	0
	$\Sigma X_1 = 0$	$\Sigma X_2 = 0$	$\Sigma X_3 = 0$

As in this case the variable X_3 (alkali source) has no numerical value, Na_2O was set as the basic activator.

Figure 1. Plackett-Burman plans. Orthogonal "half-factorial" arrangement.

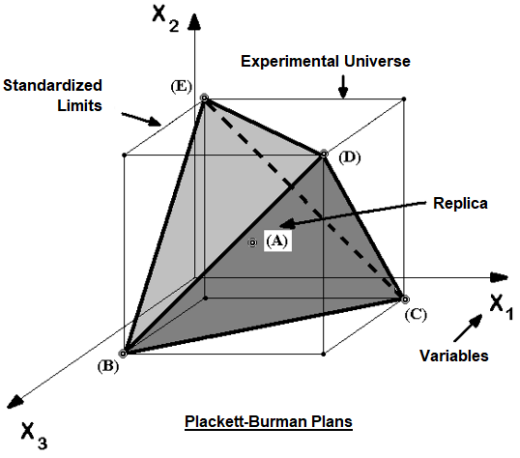

As can be seen, the influence of the other activators and the experimental error were analyzed in the experiment of the mesh center (0; 0; 0). Replacing the normalized limits with their respective values, the planning shown in Table 3 was obtained.

Table 3. Experimental Planning (MC).

EXP.	VARIABLES		
	X_1	X_2	X_3
MC1	100	0	Na_2O
MC2	100	15	Na_2O
MC3	50	0	Na_2O
MC4	50	15	Na_2O
MC5	75	7.5	Na_2O
MC6	75	7.5	Na_2O
MC7	75	7.5	Na_2O
MC8	75	7.5	K_2O
MC9	75	7.5	Na_2SiO_3
MC10	75	7.5	K_2CO_3

Sodium hydroxide (NaOH) solution is used as main alkali activator because it is widely available and less expensive.

Based on these experiments, the following regression equation was generated to study the effects of interactions between variables and second order interactions on compressive strength:

$$Y_{age} = \beta_1 X_1 + \beta_2 X_1 + \beta_3 X_1 X_1 + \beta_4 X_1^2 + \beta_5 X_1^2 \quad (2)$$

In order to follow the microstructure changes in a more comprehensive way and complement the study of experiments MC1 to MC10, pastes of BFPC and MK were also made, with and without activation by Na_2SiO_3. The contents of MK were 0, 10, 20, 50 and 70% (0-70M) in relation to the total dry agglomerate mass. The water-binding ratio was kept equal to 0.35 for pastes with 10 and 20% and equal to 0.50 for pastes with 50 and 70%. In the case of activated pastes, the Na_2SiO_3 content was kept constant and equal to 5% of the sum of the weight of MK and granulated blast furnace slag present in BFPC (50%). The activated samples were identified as 0-70MSS.

3 RESULTS AND DISCUSSION

The fact that the design of experiments reduces the sampling space, allows only a trend analysis based on the study of the limit conditions imposed by the variables, since some possible interactions are eliminated. The minimization or elimination of interactions is one of the apparent paradoxes of fractional

planning, since for the broader knowledge of the behavior of the system under study, it is necessary to observe the interactions between the variables. However, the type of experiment carried out through the half-factorial arrangements seeks to know the pure and simple additivity of the individual effects of each variable, and not the synergism between them [11]. The results obtained in the limit conditions help to identify the effects of each variable, submitted to changes in all the others, independently [11, 13].

Activation with Na_2O (Experiments MC1 to MC5)

The first part of the series of experiments, in which Na_2O was established as an activator, provided quite different strength results (Figure 2).

The MC2 experiment, containing 0% MK (upper limit of X1) and 15% Na2O (upper limit of X2), presented at 1 day of age, strength equal to that of the reference mortar (100% BFPC and without activation), experiment MC1. However, after 3 days of age, it started to show a slower rate of strength development, reaching strength at 28 days below 50% lower than that of MC1. Between 28 and 90 days of age, there was practically no strength gain, considering the scale of the error bar.

Based on these results, the following models were obtained for the ages of 3 and 28 days (eq. 3 and 4).

$$Y_{3d} = 0.5893X_1 - 1.143667X_2 + 0.116533X_1X_2 - 0.004894X_1^2 - 0.125556X_2^2 \quad (3)$$

$$Y_{28d} = 0.7143X_1 - 3.519X_2 + 0.013987X_1X_2 - 0.004146X_1^2 + 0.078644X_2^2 \quad (4)$$

Figure 2. Variation of compressive strength according to age for modified samples with different levels of MK and Na_2O. Experiments MC1 to MC5.

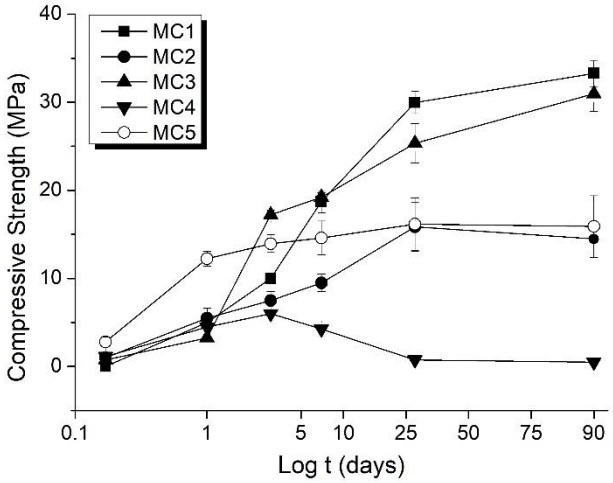

Table 4 shows the parameters of equation 2 for the other considered ages (4 hours and 1, 7 and 90 days).

Table 4. Parameters of equation 2, estimated for the other ages considered.

	4 hours	**1 day**	**7 days**	**90 days**
β_1	0.3	0.08	0.5819	0.906
β_2	0.48533	2.13167	-1.595	-4.80667
β_3	0.00084	-0.001	0.007653	0.01556
β_4	-0.003	-0.0003	-0.00395	-0.00573
β_5	-0.03351	-0.13322	0.014244	0.133156

Figures 3[a] and 3[b] shows the trends pointed out by the models, with the variation of X1 and X2, to early and to late ages, respectively.

Up to 1 day of age, alkali-activation resulted in a significant increase in the mortar's compressive strength, mainly for intermediate levels (7.5% Na_2O). In relation to MK, for 1 day of age, intermediate levels (25% MK) promoted the best results in mortar compression strength, but there was a loss of this effect when using 15% Na_2O (Figure 3 [a]). From the third day it became evident that the alkali activation by Na_2O was deleterious, especially for high MK contents (Figure 3[b]). Is clear too that even intermediary MK contents did not capable to recover the relative loss of strength.

Figure 3. Comparison between the compressive strengths of the MC1 to MC5 experiments for different ages - Trends pointed out by the obtained models. [a] 4 hours to 3 days; [b] 7 days to 28 days.

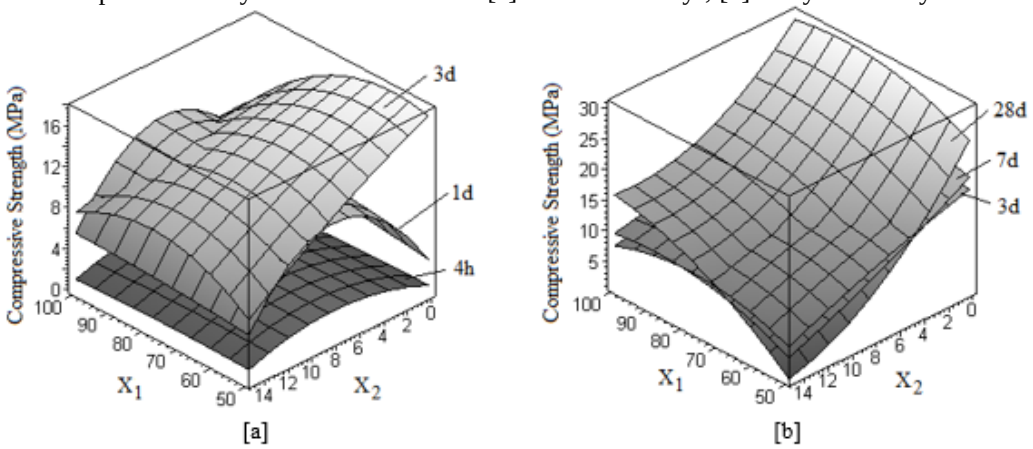

According to SILVA [14], it was concluded that high levels of alkalis in Portland cement pastes accelerate the rate of development of the initial resistance by the faster entry of silicate and aluminate ions in solution. It is known that with the increase in the concentration of these ions, their precipitation occurs on the surface of the anhydrous grains, forming an osmotic membrane that is responsible for the initial setting and hardening of the mixture.

However, in older ages the compressive strengths were reduced too much. This is attributed to the formation of greater amounts of calcium aluminate crystals, which suffer volume loss due to phase

transformations with the change in the concentration of calcium in the liquid phase. Another conclusion was that, when the alkali content is very high (> 10%), with the progress of hydration, the alkali ions in solution reach the saturation point and crystallize, generating expansive tensions and breaking the matrix continuity.

As a result of all these factors, there is a loss of strength at older ages, as confirmed by the experiment with 0% MK and 15% Na_2O (MC2), with NaOH crystals precipitated in the matrix, according to analysis by EDS - see Figure 4 [a]. The experiment without alkali-activation and with 50% MK (MC3), presented strength levels after 24 hours of hydration, equivalent to those of the reference mortar. After 3 days of age, the compressive strength achieved was 17,2 MPa, about 68% of its strength at 28 days. The strength levels reached at 3 days of age were 100% higher than those of the reference mortar (MC1). At 90 days, the compressive strength obtained was about 31 MPa, slightly lower than that of MC1, but showing an evolutionary trend.

The SEM images of the fractured surfaces of the paste with 50% MK (MC3) at 28 days of age reveal a dense microstructure, formed by the agglomeration of semi-dissolved metakaolin particles, amidst a homogeneous mass of "inner" C-S-H products, but with traces of aluminum and iron (Figure 4 [b]).

Figure 4. [a] Micrograph (SEM) of MC2 at 7 days of age. Formation of NaOH crystals, confirmed by EDS (5,000X). [b] Micrograph (SEM) of the paste with 50% MK - MC3 (1,400X).

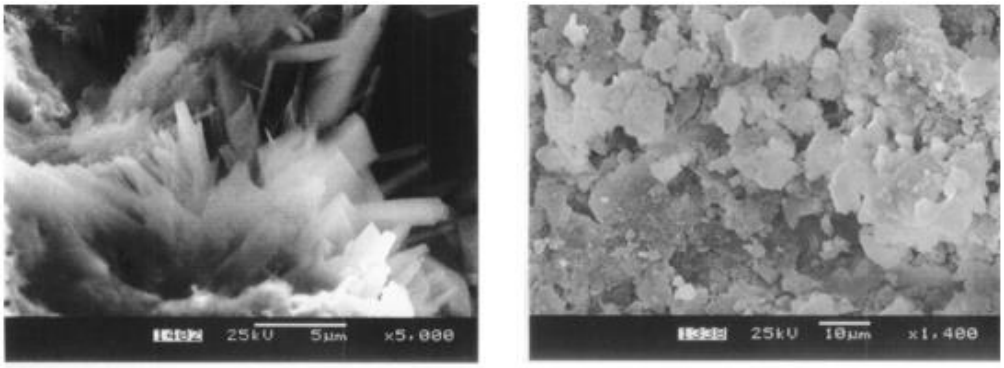

[a] [b]

The presence of these two elements suggests the formation of hydrated calcium aluminosilicate phases C-S-(A)-H, or that C-S-H has many of these adsorbed ions. No distinct crystals of calcium aluminate, ettringite or “outer” C-S-H products were found, indicating that the matrix underwent significant changes in the microstructure with the introduction of 50% MK.

According to the literature [15-18], metakaolin acts not only as a common pozzolan, that is, consuming calcium hydroxide and forming C-S-H, but also forming ettringite, calcium aluminate and C-S-(A)-H phases. This fact is due to the chemical composition of metakaolin, which contains not only active silica, but also dehydroxylated alumina. In Portland cements, the hydraulic reactivities of C_3A and C_4AF need to be controlled by the incorporation of sulfates. Small additions of calcium sulphate (< 5%) extend the pre-induction period and ensure that the start of setting only occurs at least 1 hour after adding the water.

The use of silica fume, "fly ash" and other pozzolans significantly reduces initial strength. The use of 50% addition of these pozzolans reduces the rate of strength development to very low levels, which did not happen with metakaolin.

Studies show that contents between 10 and 20% MK added promote the best results of strength and porosity [15, 19, 20]. The positive contribution of metakaolin is attributed to three elementary factors: 1) the "filler" effect, 2) the acceleration of the hydration of Portland cement and 3) the pozzolanic reaction with calcium hydroxide. The filler effect is related to the fineness of the metakaolin, whose average particle size is generally around 5 μm. The acceleration of hydration is attributed to the aluminum present in the metakaolin.

Significant strength gains have been reported for the first 48 hours of hydration using metakaolin and that such gains were proportional to the fineness of this material [16, 19]. Several authors have also reported an increase in the rate of hydration heat release with the addition of metakaolin, that the maximum increase occurred when the addition content was around 10% in relation to the cement mass and that the maximum exothermic peaks occurred in the first 48 hours of hydration [16-18]. These observations initially surprised the researchers, since the use of pozzolans generally reduces the heat of hydration, a phenomenon considered potentially harmful to large volume concrete structures (mass concrete) [6].

Another point cited is that the positive contribution of metakaolin to resistance does not continue after 14 days of hydration, regardless of the replacement content [20]. This is supposed to result from a change in the kinetics of the reactions between metakaolin and calcium hydroxide after 14 days [20].

The metakaolin is similar to silica fume in some aspects, particularly regarding the specific surface (> 1,000 m^2/kg) and also because it contains silica, whose reaction with $Ca(OH)_2$ produces more C-S-H gel. However, metakaolin also contains alumina, which in the reaction produces additional crystalline phases containing alumina. According to the literature, hydrated calcium aluminate ($4CaO{\cdot}Al_2O_3{\cdot}13H_2O$) or abbreviated ($C_4AH_{13}$) and ($C_3AH_6$) and strätlingite, a hydrated calcium aluminosilicate (C_2ASH_8), are the main phases identified [17-19].

As for the final porosity of the hardened paste, the use of metakaolin causes a refinement in the pore structure [19, 20]. Another fact described in the literature is the sudden increase in porosity that occurs at 14 days of age in mixtures containing 5 to 15% addition of metakaolin [19].

Studies carried out on pastes containing mixtures 1: 1 metakaolin and lime, cured in a humid chamber at 40 ºC indicate that the initial hydration products are the C-S-H gel, C_4AH_{13}, strätlingite (C_2ASH_8) and subsequently C_3AH_6. It has been suggested that porosity increases in this period due to the transformation of C_4AH_{13}, of hexagonal structure, to C_3AH_6, of cubic structure [5, 7, 19]. The packaging generated by the phase transformation generates a decrease in the volume of solids and, consequently, an increase in porosity [19]. As the hydration process is continuous, and both phenomena occur simultaneously, resistance gain was not recorded in this period. After 28 days, the porosity drops again due to the continuity of the hydration process.

The results of X-ray diffraction analyzes of the paste with 50% MK (MC3) indicated that there was no formation of $Ca(OH)_2$ (portlandite), but revealed the presence of $Ca_6Al(SO_4){\cdot}3(OH)_{12}{\cdot}26H_2O$ (ettringite), $Ca_2Al(OH)_7{\cdot}3H_2O$, $4CaO{\cdot}Al_2O_3{\cdot}13H_2O$ (hydrated calcium aluminate – strätlingite), as well as $CaCO_3$ (calcite) and remaining C_2S (Figure 5).

Figure 5. X-ray diffractogram of the paste with 50% MK (MC3), after 28 days of hydration.

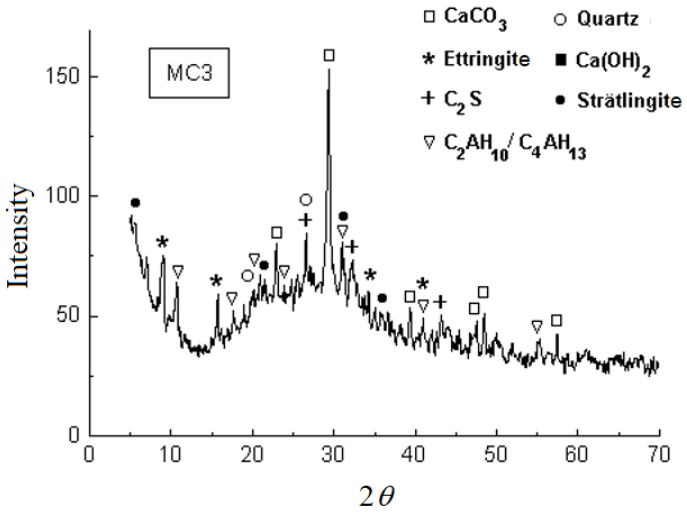

The presence of calcite in hydrated Portland cement is common, as in many cases this product is used as a "filler" (limestone filler) to alleviate the effects of autogenous retraction [5]. However, it is known that part of the calcium hydroxide (portlandite) generated during hydration can undergo carbonation by contact with atmospheric air. Therefore, as the diffractogram did not show the presence of portlandite, or there was total carbonation, or the calcite present in the sample comes only from the limestone filler. As previous studies have revealed that the addition of metakaolin accelerates the carbonation kinetics of $Ca(OH)_2$, the first hypothesis is more plausible [18].

The formation of crystalline C-S-(A)-H phases was confirmed by the presence of diffraction peaks identified by the strätlingite pattern ($Ca_2Al_2SiO_7$ $8H_2O$).

The DSC results confirm the microstructural changes that occurred with the addition of 50% MK (Figure 6).

For the reference sample (MC1), the DSC curve shows two main endothermic peaks. The first, at about 150 ºC, is reported in the literature to include the transitions that occurred in the C-S-H, AFt and AFm phases due to the removal of free, adsorbed water and also the structural water of these compounds [6]. The second peak, at about 480 ºC, occurred due to the dissolution of portlandite.

A third transition, which did not occur in the sample with 0% MK (MC1), but which occurred in the sample with 50% MK (MC3) is related to the dissolution of $CaCO_3$ which generates an endothermic peak at around 800 ºC [19, 20]. The shift to the left and the reduction of the first endothermic peak are related to the phases AFm (C_4AH_{13}, C_2AH_{10} and monosulfate), AFt (ettringite), strätlingite and C-S-(A)-H, formed in detriment to C-S-H [3, 5]. The absence of the second endothermic peak in the DSC of the sample with 50% metakaolin (MC3) corroborates the results of the X-ray diffraction analyzes, confirming the absence of portlandite. However, it is possible that part of the portlandite generated by the hydration of Portland cement has not been consumed by pozzolanic reactions and has undergone carbonation.

Figure 6. DSC curves for pastes with 0% MK and 50% MK - MC1 and MC3, respectively.

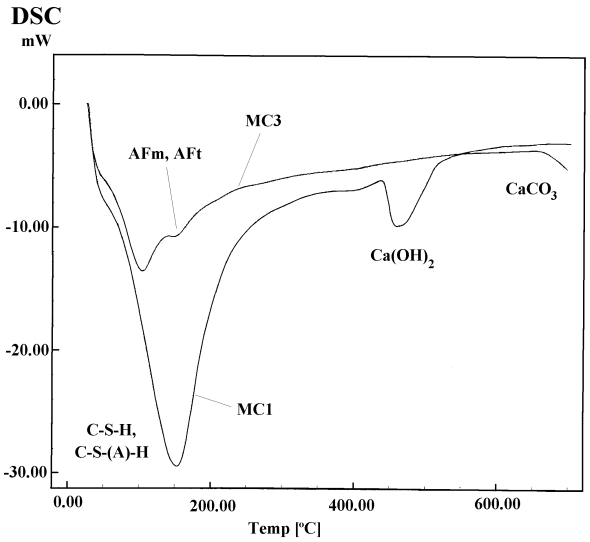

Hence, it is likely that the drop in the rate of development of compressive strength in later ages is related to a greater number of AFm and AFt phases formed, to the detriment of C-S-H [4, 21, 22].

As for the alkali activation of mixtures containing metakaolin, the MC4 experiment (50% MK and 15% Na_2O) revealed results below expectations. It was believed that the presence of alkalis in the solution would further increase the reactivity of MK. The pH equal to 11, recorded in this experiment shortly after mixing, did not cause an increase in initial resistances. At 1 day of age, the compressive strength values were similar to the reference values. From the third day of hydration, gradual losses of resistance were recorded. However, there was not macroscopically any indication of expansive stresses and breakdown of sand particles.

SEM analysis of these pastes (MC4) at 7 days of age revealed a heterogeneous microstructure, quite different from that presented by the paste with 50% MK and without activation (MC3), where small acicular crystals rich in aluminum and calcium, but without traces sulfur, appear in the middle of a porous mass of C-S-H and C-S-(A)-H phases. In aluminous cements (CACs), the formation of this phase, identified as CAH_{10}, is common, especially when the Al_2O_3/CaO ratio in cement is high. These hexagonal aluminates are also unstable and are transformed into C_2AH_6 during hydration [4, 21].

The high sodium content detected by EDS suggests that these ions are combined in the structure of C-S-(A)-H and not only adsorbed on its surface. Figure 7 [a] shows details of the formed microstructure. The high porosity presented by the microstructure, and the presence of a large quantity of hydrated calcium aluminate crystals, confirm the possibility of the gradual reduction in strength being caused by the eventual volume loss associated with the phase transformations that occurred in these compounds. According to the literature [5, 7, 9], alkali ions in high concentration in the liquid phase contribute to the formation of AFm phases like CAH_{10}, C_4AH_{13} and C_2AH_{10}, while reducing the formation of ettringite.

The MC4 X-ray diffractogram after 28 days of age is shown in Figure 7[b]. The results also reveal the absence of portlandite and the formation of ettringite and calcium aluminates, as well as strätlingite and remaining C_3S, in addition to C_2S, confirming the SEM analysis. It is likely that the CAH_{10} diffraction peaks have been confused with those generated by the other aluminate phases [4].

The formation of NaOH crystals was not detected, as occurred in the paste with 0% MK and activated with 15% Na_2O - MC2 (Figure 4 [a]), indicating that all the sodium present is combined or adsorbed in the hydrated phases.

The porosity of the microstructure shown in Figure 7 [a] is related to the reduction of the metakaolin solubility, as well as to the structural instability of the formed aluminate phases and the probable formation of delayed ettringite. The presence of C_2S and C_3S indicates that the hydration of the cement was delayed. As the mixing water was less "hard" with the addition of alkalis, the consistency obtained in the paste with 50% MK was considered satisfactory, even though the water/binder ratio was kept constant. However, it is possible that the dispersion of the particles was impaired when incorporating the MK and that the water content was not sufficient to guarantee the total hydration of the mixture.

The experiment with 25% MK and 7.5% Na_2O (MC5), showed better results of early strength. At 1 day of age the average compressive strength achieved was twice that of the reference mortar. However, as of the third day of hydration, the resistance gain was minimal, equivalent to the results of the experiment with 0% MK and 15% Na_2O (MC2).

Figure 7. [a] Micrograph (SEM) of the paste with 50% MK and 15% Na_2O (MC4) at 7 days of age. Detail of the formation of aluminate phases type CAH_{10} (10,000X). [b] X-ray diffractogram, at 28 days of age.

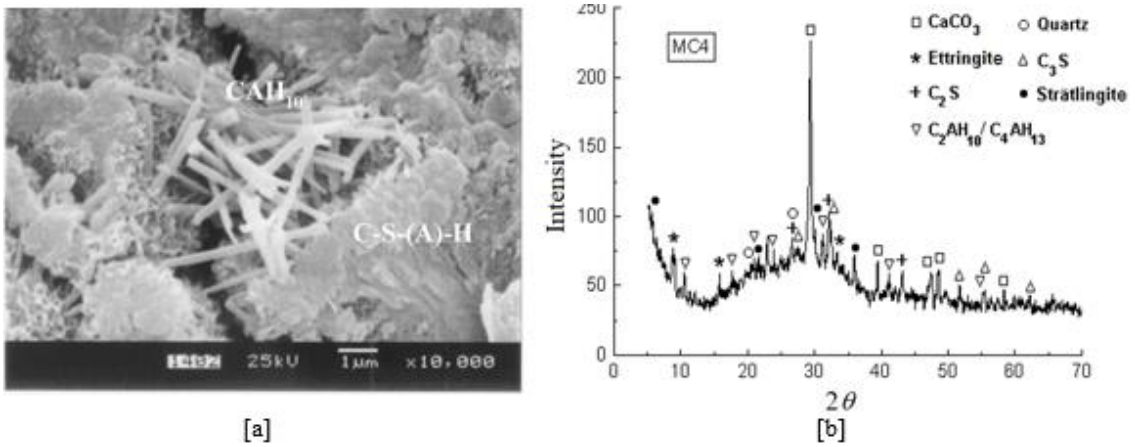

[a] [b]

The microstructure images at 7 days of age revealed the formation of lamellar crystals randomly arranged among themselves, on the C-S-H and/or C-S-(A)-H matrix. EDS analyzes of these crystals showed high levels of calcium (62%) and silicon (20.5%) and traces of aluminum (16.2%) and sodium (1.3%). Figure 8 [a] shows details of the formed microstructure.

As expected, the lower content of MK, associated with alkali activation ensured the formation of a more compact and homogeneous microstructure. There was a considerable increase in compressive strength until 3 days of age, but from then on, there was no evolution (Figure 2). It is assumed that, at ages over 3 days, the volumetric variation resulting from the transformations of the AFt and AFm phases has contributed negatively to the strength. As the Na_2O content was lower than in the MC2 (7.5%), there was no crystallization in the matrix and, with that, there was no gradual loss of resistance at older ages. It is also likely that the continuous formation of hydration products has compensated for any damage caused by the AFt and AFm phases, guaranteeing the stability of the strength. The X-ray diffractogram of the MC5 sample is shown in Figure 8 [b].

Figure 8. [a] Micrograph (SEM) of the paste with 25% MK and 7.5% Na_2O (MC5) at 28 days of age. Details of hydrated calcium silico-aluminate particles morphology (5,000X). [b] Respective X-ray diffractogram.

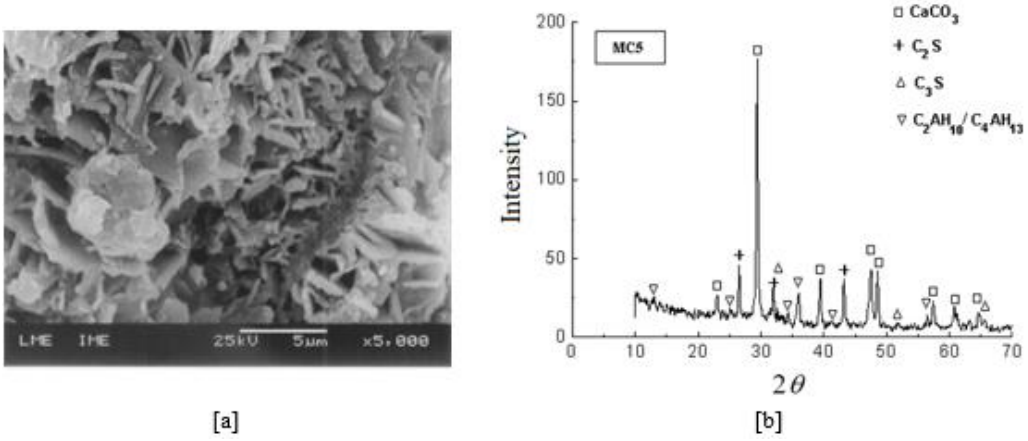

The results of X-ray diffraction confirm the microscopic analysis, showing the presence of aluminates and the absence of portlandite and ettringite.

The MC6 and MC7 experiments are replicas of the MC5 and served to evaluate the experimental error. Table 4 shows the results obtained in these experiments.

Table 4. Compressive strength results presented by replicas of the MC5 Experiment.

Exp	Age (days)	σ_c (MPa)	SD (MPa)	CV(%)
MC5	1	12.24	0.58	4.71
	3	14.48	0.46	3.15
	7	13.74	0.46	3.32
	28	16.48	1.51	9.17
MC6	1	12.24	0.20	1.67
	3	14.36	0.25	1.74
	7	15.73	0.87	5.50
	28	15.23	1.32	8.67
MC7	1	12.24	0.50	4.08
	3	12.99	0.64	4.97
	7	14.30	1.54	10.80
	28	16.73	1.10	6.56

σ_c – Compressive strength; SD - Standard deviation; CV – Coefficient of variation.

The dispersion measures for the MC5, MC6 and MC7 experiments that indicate the experimental error, were considered satisfactory.

Comparisons between types of activator (MC5 to MC10).

The MC8, MC9 and MC10 experiments, with the same MK content (25%) and activator content (7.5%), but with different types of activator, K_2O, Na_2SiO_3 and K_2CO_3, respectively, showed similar rates of development resistance, up to 3 days old. After 7 days, the results of compressive strength obtained were all different, but still higher than those of MC5, with Na_2O (Figure 9).

Figure 9. Variation of compressive strength according to age. Experiments MC1 (reference) and MC5 to MC10 (25% MK and 7.5% different types of alkali activator).

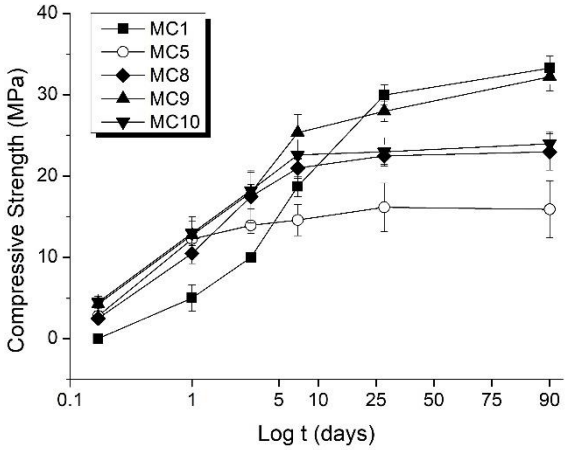

The experiments with 25% MK and 7.5% K_2O (MC8) and with 25% MK and 7.5% K_2CO_3 (MC10), which showed very close compressive strength values, also developed similar microstructures. The images obtained by SEM revealed massive formation of C-S-H and C-S-(A)-H products with high potassium levels (~ 8%). Small lamellar particles with rounded edges also occurred throughout the matrix (Figure 10 [a]).

The semi-quantitative chemical analysis of these particles (obtained by EDS) showed the following average composition: 51.8% CaO, 13% SiO_2, 26.1% Al_2O_3 and 8.3% K_2O. The high aluminum content indicates the formation of hydrated calcium and potassium aluminate phases, and the high affinity of this element to replace calcium in the hydrated phases. Figure 10 [b] shows the X-ray diffractograms of the samples MC8 and MC10.

In the experiment with 25% MK and 7.5% Na_2SiO_3 (MC9), which showed the best results in compressive strength, a small reduction in the rate of resistance development was detected between 7 and 28 days, but after 28 days the rate initial resumption.

As shown in Figure 9, at 1 day of age, the levels of compressive strength achieved by the MC9 were three times the reference experiment (MC1). At 28 days, MC1 and MC9 reached very close levels and, at 90 days, MC9 showed about 10% more compressive strength.

Figure 10. Micrographs (SEM) of the microstructures typical developed by the MC8 and MC10 pastes. Porous microstructure (1,400X). [b] X-ray diffractogram of the respective samples.

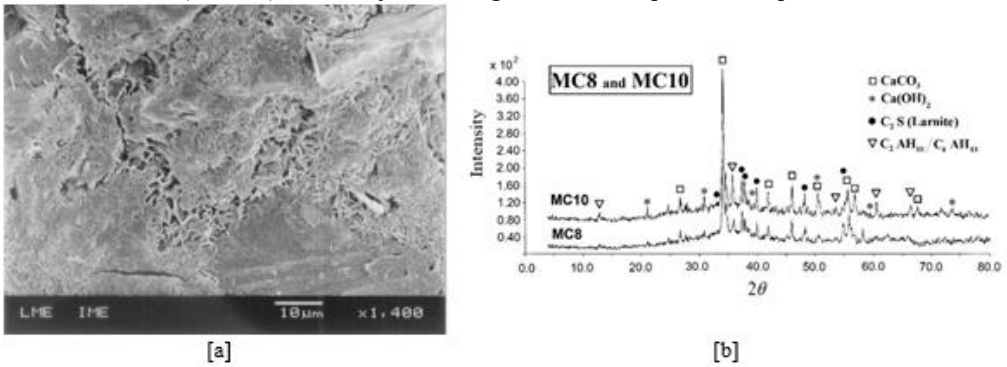

The details of the fractured surfaces of these pastes, at the age of 28 days, are shown in Figure 11 [a]. The micrographs reveal the formation of short needle crystals radiating from the matrix, rich in SiO_2, CaO and Al_2O_3, but also showing traces of Fe_2O_3, SO_3 and alkalis, as detected by EDS. Portlandite crystals are still found in the microstructure, but showing an irregular morphology, suggesting that they are being consumed by reactions with MK. The X-ray diffractogram of the paste with 25% MK and 7.5% Na_2SiO_3 (MC9) at 28 days of age is shown in Figure 11 [b]. $CaCO_3$, C_2AH_{10}, portlandite, ettringite (delayed) and C_2S were identified again (larnite).

Figure 11. [a] Micrographs (SEM) of the paste with 25% MK and 7.5% Na_2SiO_3 (MC9) at 28 days of age. Presence of ettringite crystals radiating from the matrix of C-S-H and C-S-(A)-H, and detail of a portlandite crystal partially consumed by pozzolanic reactions. [b] X-ray diffractogram of the MC9 at 28 days of age.

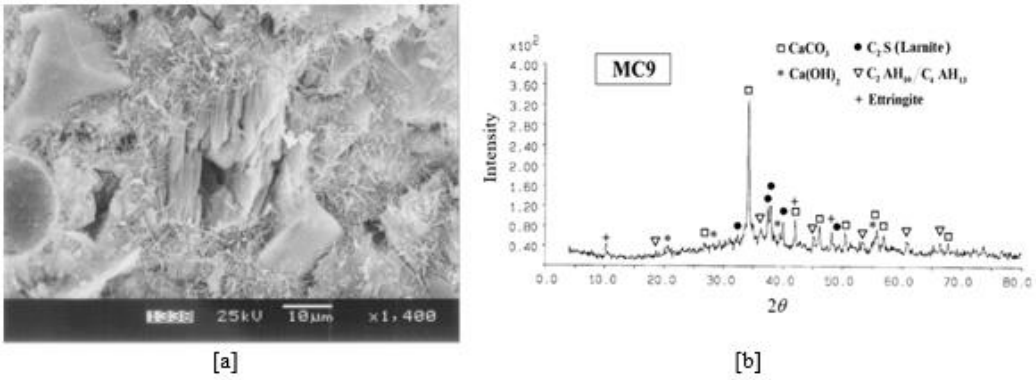

[a] [b]

According to the compressive strength results, it is likely that between 28 and 90 days, the remaining portlandite was consumed to form more C-S-H and C-S-(A)-H from MK. Another assumption is that, because it contains silica, the activator Na_2SiO_3 functioned as pozzolan, promoting the formation of more C-S-H and C-S-(A)-H phases and contributing to the maintenance of better mechanical stability [23]. For a definitive conclusion, it is necessary to analyze the evolution of the microstructure as a function of time until more advanced ages.

Analysis of pastes with intermediate contents of metakaolin (MK), not activated and activated by sodium silicate (SS)

The analysis of pastes with 10 to 70% of MK, not activated and activated with 5% wt/wt Na_2SiO_3 (SS), provided very conclusive results. The paste containing 10% addition of MK and without activation (10M) showed, at 28 days of age, massive microstructure, with high levels of Al and Si and Ca, according to analysis by EDS. Hydrates of acicular morphology emerge from the surface, which may be “outer” C-S-H or ettringite, since traces of sulfur were detected (Figure 12 [a]).

The addition of 5% Na_2SiO_3 caused a slight change in the microstructure (10MSS). The matrix composed of C-S-H and/or C-S-(A)-H seems less compact and with a low degree of solubilization. It is possible to notice the formation of shorter and evenly distributed ettringite crystals throughout the matrix. Figure 12 [b] shows details of the formed microstructures.

Figure 12. Micrographs (SEM) of the pastes containing: [a] 10% MK (10M). [b] 10% MK and 5% Na_2SiO_3 (10MSS) – Both showing formation of massive hydrated products and ettingite fibrils (1,400X).

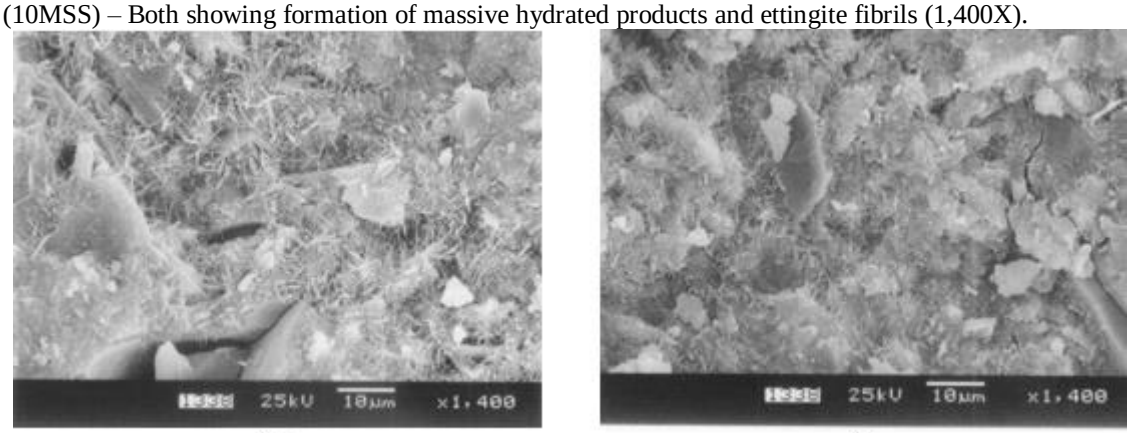

[a] [b]

The DSC curves of the 10M and 10MSS pastes are shown in Figure 13. There was a small variation in the intensity of the endothermic peak associated with C-S-H, caused by the formation of more phases AFt and AFm. The lower intensity of the portlandite dissolution peak reveals that this phase was consumed to form C-S-H or C-S-(A)-H. The curves also show a tendency for significant differences between the endothermic peaks associated with the dissolution of $CaCO_3$. However, the available equipment did not allow analysis of the transitions at higher temperatures.

Figure 13. DSC curves for 10M and 10MSS pastes.

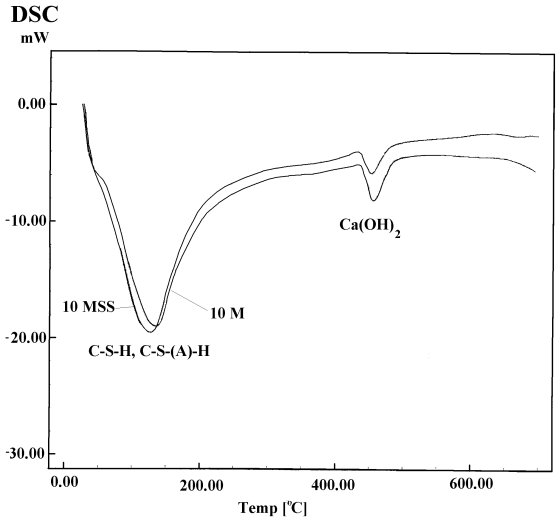

The addition of 20% MK and without alkali activation (20M), became more evident the influence of pozzolan in the formation of delayed ettringite. At 28 days, there is still a large amount of these crystals covering the entire fracture surface. Figure 14 [a] shows images of the developed microstructure. The rupture occurred through the ettringite crystals, which are relatively weaker than the C-S-H matrix, revealing regions where there is a higher concentration of these crystals and, consequently, more high porosity.

The paste with 20% MK and 5% Na_2SiO_3 (20MSS) also showed formation of ettringite, but in

lower concentration. It was also noted that there was only a partial solubilization of the MK particles, suggesting that the alkali activation caused a reduction in the wettability of these particles. Figure 14 [b] shows micrographs of the 20MSS paste, at 28 days of age.

The results of the analysis of the paste with 50% MK and without alkali activation (50M) have already been presented and discussed in relation to the MC3 experiment, since the samples are identical. In the activation of these pastes, with 5% Na_2SiO_3 (50MSS) the micrographs showed the formation of a microstructure quite different from that presented by the experiment with 50% MK and 15% Na_2O (MC4) (Figure 15 [a]). Small crystals of hydrated calcium aluminate (C_4AH_{13} and C_2AH_{10}) occurred on the surface of large agglomerates formed by semi-dissolved MK particles and a porous mass rich in Ca, Si and Al, probably C-S-(A)-H. No acicular crystals of CAH_{10} were found as seen in MC4. Again, a reduction in compactness was noted when compared to the not activated sample (50M).

Figure 14. Micrographs (SEM) of the pastes containing: [a] 20% MK and 5% Na_2SiO_3 (20MSS). [b] 20% MK and 5% Na_2SiO_3 (20MSS) – Again, delayed ettingite crystals covering all microestructure (1,400X).

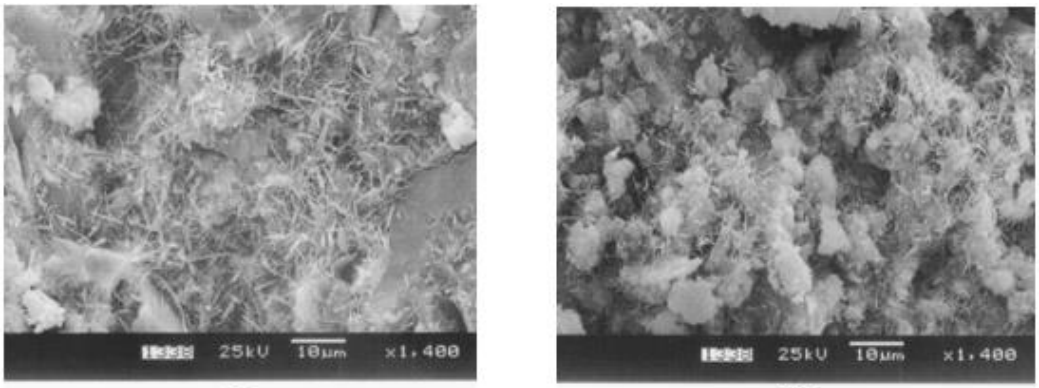

[a] [b]

The paste with 70% metakaolin showed a low degree of solubilization (70M). However, ettringite formation was still detected among unreacted grains, which was probably responsible for the mixture hardening. The details of the microstructures formed at 28 days are shown in Figure 15 [b].

Figure 15. Micrographs (SEM) of the pastes containing: [a] 50% MK and 5% Na_2SiO_3 (50MSS). Porous microstructure formed by large particleboard (1,400X); [b] 70% MK (70M). Microstructure formed by the agglutination of partially dissolved particles and ettringite crystals (1,400X).

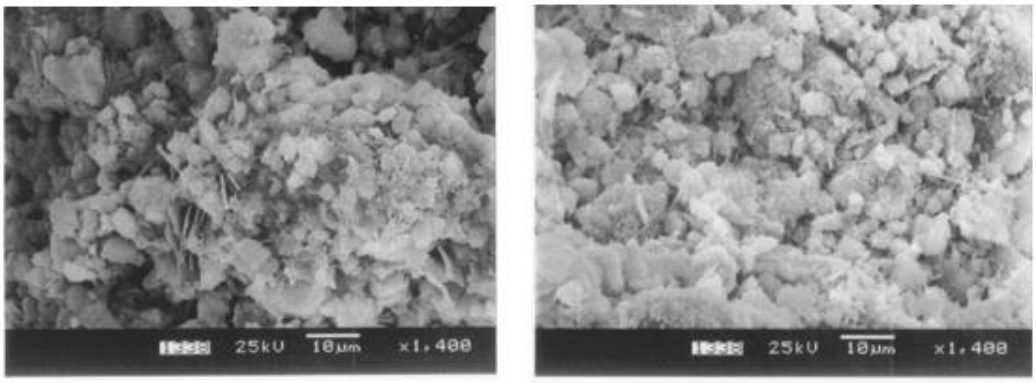

[a] [b]

The unreacted metakaolin particles are easily identified in the microstructure, but the analysis by EDS reveals traces of calcium in its composition. As this analysis detects elements on the sample surface, it is assumed that the calcium signal is due to the presence of the precipitated hydroxide on the surface of the MK grain.

The paste with 70% MK and 5% Na_2SiO_3 (70MSS) showed an even lower degree of solubilization, even at 28 days of age (Figure 16 [a]). Comparing the micrographs of the 70M and 70MSS pastes, the influence of the presence of the activator is clear.

As previously discussed, the presence of alkalis reduces the solubility of CaO, however it increases the diffusivity of hydroxyl ions and the addition of metakaolin accelerates the initial hydration of Portland cement since it also has reactive alumina in its composition.

According to the literature [15], electrical conductivity data obtained indicate that the ionic concentrations and the mobilities of Ca^{2+}, OH^-, SO_4^{2-}, Na^+ and K^+ ions decrease rapidly after the initial hydration of Portland cement. These ions are rapidly adsorbed by the formation of a thin layer of hydration products, which forms a shell around the anhydrous cement particles functioning as an osmotic membrane, as discussed earlier. This shell consists of double-charged layers of adsorbed calcium ions and other ionic species that lead to a decrease in both the number and mobility of the ions, reducing the rate of hydration.

The microstructure formed in 70MSS paste is similar to that observed in Portland cement pastes with few hours of hydration.

As the activator Na_2SiO_3 has 35.6% of SiO_2 in its composition, when added to the mixture, it also contributes to the modification of the molar ratios between silica and other compounds. Figure 16 [b] shows the variation of the SiO_2/Al_2O_3 and SiO_2/CaO ratios, depending on the content of addition of MK and Na_2SiO_3 activator.

It is possible to clearly see the increase in the content of Al_2O_3 with the addition of MK. The influence of the activator as a supplemental source of silica is also evident. If the SiO_2/CaO ratio is taken as an index of reactivity, it is clear to conclude why the pozzolanic activity falls too low for high levels of pozzolan addition, as indicated by the compressive strength results and the microstructures discussed previously. Since the pozzolanic reaction occurs between the silica from the pozzolan and the calcium hydroxide released during the hydration of the Portland cement silicates, the higher the SiO_2/CaO ratio, the lower the reactivity of the mixture.

Figure 16. [a] Micrograph (SEM) of the pastes containing 70% MK and 5% Na_2SiO_3 (70MSS). Open microstructure, showing a low degree of hydration and agglutination of the MK particles (1,400X); [b] Variation of SiO_2/Al_2O_3 and SiO_2/CaO molar ratios with MK content.

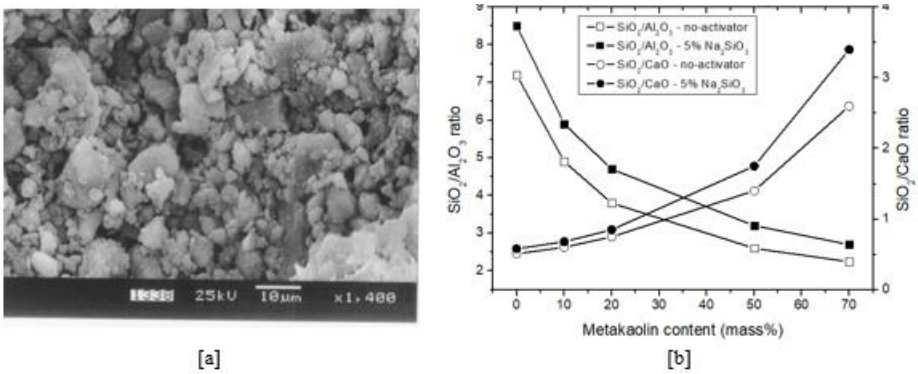

Figure 17 [a] shows the evolution of the DSC curves with the MK content. Even for low levels of addition, the DSC results show a marked reduction in the intensity of the first endothermic peak (100-150 ºC), indicating that there was a reduction in C-S-H or C-S-(A)-H products. However, the addition of metakaolin caused greater formation of calcium aluminate phases and also increased the aluminum content in the matrix. Metakaolin promoted the formation of type C-S-(A)-H phases and these showed water loss at lower temperatures (100-130 ºC).

For contents of 50 and 70% of MK (samples 50M and 70M), the reduction in the intensity of the first endothermic peak, revealed the occurrence of a new transition at about 150 ºC, nonexistent or superimposed by the main peak for contents from 0 to 20% metakaolin. According to the literature, this peak is related to the dissolution of the hydrated calcium aluminate phases, mainly of C_4AH_{13} [16]. Similar transitions are also reported in the literature with respect to CAH_{10} fibrous crystals, which occur in aluminous cements [5, 9].

In the second main peak, associated with the dissolution of portlandite, there was a continuous reduction in its intensity with an increase in the metakaolin content. In the sample with 20% MK (20M), there was a reduction in the peak of portlandite (between 450 and 500 ºC), compared with the sample with 10% MK (10M), and also greater formation of C-S-H. The DSC curves for samples 50M and 70M showed no indication of the presence of portlandite.

For samples activated with 5% Na_2SiO_3 (10MSS to 70MSS), the DSC curves also showed a marked reduction in the intensity of the endothermic peaks (Figure 17 [b]). Comparing the 10MSS and 20MSS samples, in the latter there was a greater reduction in the portlandite peak, but there was also less C-S-H formation.

Figure 18 [a] shows the evolution of X-ray diffractograms as a function of the MK content of not activated samples. The results confirm the previous observations, about the formation of ettringite and hydrated calcium aluminates and the reduction of the formation of portlandite. The XRD spectra also show the possible formation of strätlingite. Figure 18 [b] shows the evolution of the X-ray diffraction spectra for samples activated with 5% Na_2SiO_3. For the activated sample, with 0% MK (0MSS), the results show that there was low consumption of C_2S and C_3S, indicating that Na_2SiO_3 delayed its hydration.

With the increase in the MK content, there was a reduction in the intensity of the reflections of these compounds, indicating a higher degree of dissolution. Another evidence was the intensity of the portlandite peaks, which increased in the 10MSS sample, compared to the reference sample (0MSS). The formation of ettringite and hydrated calcium aluminates with hexagonal structure was also confirmed. Although marked in the XRD spectra, it was not possible to conclude with accuracy if there was formation of strätlingite, since its characteristic peaks coincide with those of other AFm phases.

Another fact evidenced by the results is the marked presence of $CaCO_3$ in all samples analyzed. This fact reinforces the hypothesis of the occurrence of alkaline hydrolysis, where alkalis catalyze the formation of $CaCO_3$ from hydrated calcium aluminates [20]. It is supposed that metakaolin also contributes to the formation of $CaCO_3$, since it is an extra source of aluminum for the formation of hydrated calcium aluminates.

Figure 17. [a] Micrograph (SEM) of the pastes containing 70% MK and 5% Na_2SiO_3 (70MSS). Open microstructure, showing a low degree of hydration and agglutination of the MK particles (1,400X); [b] Variation of SiO_2/Al_2O_3 and SiO_2/CaO molar ratios with MK content.

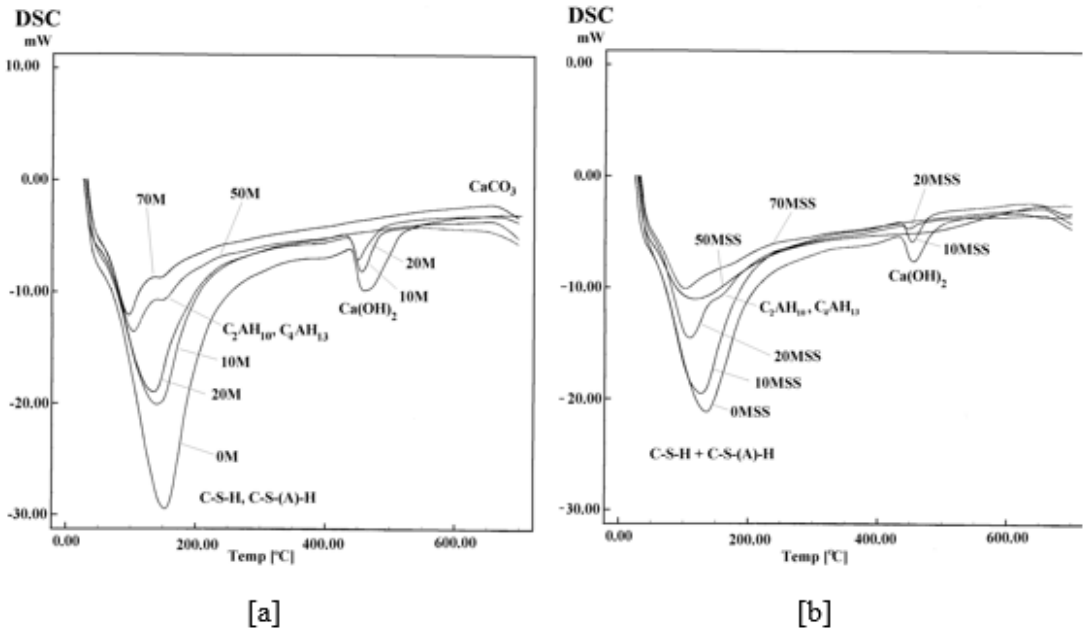

Figure 18. X-ray diffractograms of samples, containing: [a] 0 to 70% MK (not activated); [b] 0 to 70% MK and activated with 5% Na_2SiO_3.

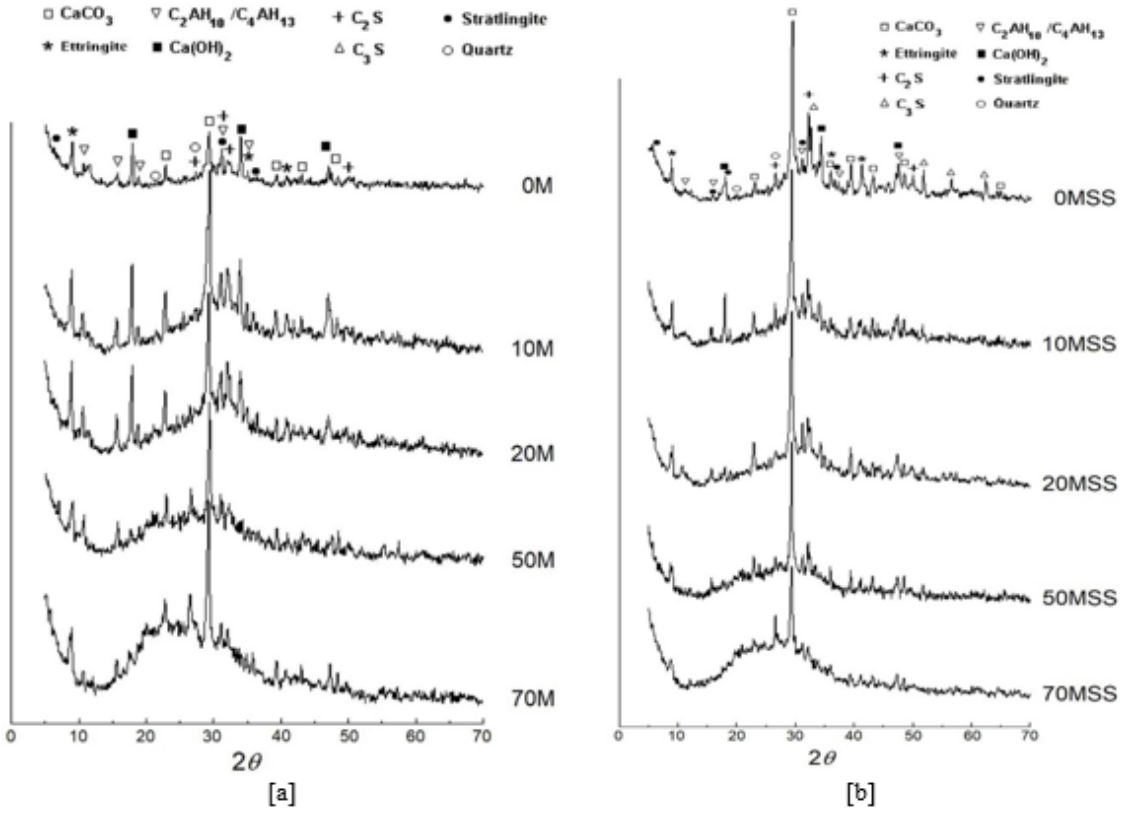

4 CONCLUSIONS

Half-factorial planning allowed to analyze trends and identify the best conditions for combining the chosen reagents. The results clearly showed the influence of the MK pozzolanic activity and the type and content of activator used, in the development of compressive strengths of BFPC-MK blends.

The use of MK accelerates the hydration of Portland cement silicates, because it has aluminum in its composition. High initial strengths are obtained for addition contents of 50% MK. The consumption of portlandite and the extra formation of C-S-(A)-H phases are the main positive effects registered. However, MK also promotes the formation of ettringite and unstable hydrated calcium aluminate phases, which, with the progress of hydration, undergo a change in structure and volume loss, contributing to the reduction of final strengths.

Alkali activators, when incorporated into the mixture, reduce the solubility of calcium and in contact with the MK, contribute to the formation of more hydrated calcium aluminate phases and to the reduction of the formation of delayed ettringite. However, the alkalis do not prevent the phase transformations of the CAH_{10}, C_2AH_{10}, C_4AH_{13} to C_2AH_6 aluminates to occur and, as a result, the loss of mortar compression strength in older ages is even greater. For samples with contents above 10%, alkalis crystallize amidst the hydrated phases, breaking the matrix continuity, reducing the mechanical strength. Among the alkali activators, sodium silicate (Na_2SiO_3) provided the best results in compressive strength. Because it is a silicate, silica is supposed to have contributed to reducing the formation of unstable aluminates by the formation of strätlingite and C-S-(A)-H products.

ACKNOWLEDGEMENTS

The authors would like to thank CAPES and CNPq for the financial support to students (scholarships), IME for the analyzes by SEM/EDS and DSC, and PUC-Rio for the analyzes by XRD, and the reviewers for the suggestions that improved the quality of this work.

REFERENCES

[1] PROVIS J. L, "Alkali activated materials". *Cement and Concrete Research*, v. 114, pp:40-48, 2018.

[2] ABDOLLAHNEJAD, Z.; HLAVACEK, P.; MIRALDO, S.; PACHECO-TORGAL, F. "Compressive strength, microstructure and hydration products of hybrid alkaline cements", *Materials Research*, v. 17, n. 4, pp: 829-837, 2014.

[3] ROY, S.; CHANDA, S. K.; BANDOPADHYAY, S. K.; GHOSH, S. N. "Investigation of Portland slag cement activated by waterglass". *Cement and Concrete Research*, v. 28, n. 7, pp. 1049-1056, 1998.

[4] MANSUR, L. F.; SANTANA, C. M. A.; PIRES, E. F. C.; ABREU, F. L. B.; MOUNZER, E. C.; SILVA, F. J. "Microestrutura e propriedades físicas e mecânicas de cimento Portland tipo II álcali-ativado". *Brazilian Journal of Development*, v. 6, n. 11, pp.84929-84951, 2020.

[5] ODLER, I. "Hydration, setting and hardening of Portland cement", In: Peter C. Hewlett. (ed), *Lea's Chemistry of Cement and Concrete*, 4 ed,London, UK, Elsevier, 2004.

[6] SCRIVENER, K. L.; JOHN, V. M.; GARTNERC, E. M. "Eco-efficient cements: potential economically viable solutions for a low-CO_2 cement-based materials industry", *Cement and Concrete Research*, v. 114, pp. 2-26, 2018.

[7] Bernal, S. A.; Gutierrez, R. M.; Rodríguez, E. D. "Alkali-activated materials: cementing a sustainable future", *Ingeniería y Competitividad*, v. 15, n. 2, pp. 211-223, 2013.

[8] LUUKKONEN, T.; ABDOLLAHNEJAD, Z.; YLINIEMI, J.; KINNUNEN, P.; ILLIKAINEN, M. "One-part alkali-activated materials: a review", *Cement and Concrete Research*, v. 103, pp. 21–34, 2018.

[9] ALASTAIR, M.; ANDREW, H.; PASCALINE, P.; MARK, E.; PETE, W. "Alkali activation behaviour of un-calcined montmorillonite and illite clay minerals", *Applied Clay Science*, v. 166, pp. 250–261, 2018.

[10] BAJZA, A.; ROUSEKOVÁ, I. ZIVICA, V. "Silica fume-basic blast furnace slag systems activated by Na alkali silica activator", *Cement and Concrete Research*, v. 27, n. 2, pp. 1825-1828, 1997.

[11] VILLAS-BÔAS, R. *"Arranjos ortogonais de taguchi: os Ln(2k)"*, Série qualidade e produtividade. CETEM/CNPq, 1996.

[12] WEISER, M. W.; FONG, K. B.; "Application of the taguchi method of experimental design to improving ceramic processing", *Engineering*, v. 73, n. 1, pp. 83-86, 1994.

[13] CLARK, G., M. "*Statistics and experimental design*", Edward Arnold, 2 ed, 1980.

[14] SILVA, F. J. "*Reforço e fratura em compósitos de matriz álcali-ativada*", Tese de Doutorado, IME, 2000.

[15] KARATAS, M.; DENER, M.; MOHABBI, M.; BENLI, A. "A study on the compressive strength and microstructure characteristic of alkali-activated metakaolin cement", *Revista Matéria*, v. 24, n. 4, e-12507, 2019.

[16] MORSY, M. S.; EL-ENEIN, S. A.; HANNA, G. B. "Microstructure and hydration characteristics of artificial pozzolana-cement pastes containing burnt kaolinite clay, *Cement and Concrete Research*, v. 27, n. 9, pp. 1307-1312, 1997.

[17] GERALDO, R. H.; OUELLET-PLAMONDON, C. M.; MUIANGA, E. A. D.; CAMARINI, G. "Alkali-activated binder containing wastes: a study with rice husk ash and red ceramic", *Cerâmica*, v. 63, pp. 44-51, 2017.

[18] AMIN, M. S.; ABO-EL-ENEIN, S. A.; RAHMAN, A. A.; ALFALOUS, K. A. "Artificial pozzolanic cement pastes containing burnt clay with and without silica fume: physicochemical, microstructural and thermal characteristics", *Journal of Thermal Analysis and Calorimetry*, v. 107. n. 3, pp. 1105-1115, 2012.

[19] TORRES-CARRASCO, M.; PUERTAS, F. "Alkaline activation of different aluminosilicates as an alternative to Portland cement: alkali activated cements or geopolymers", *Revista Ingeniería de Construcción*, v.32, n. 2, 2017.

[20] RAHIM, R. H. A.; RAHMIATI, T.; AZIZLI, K. A.; MAN, Z.; NURUDDIN, M. F.; LUKMAN, I. "Comparison of using NaOH and KOH activated fly ash-based geopolymer

on the mechanical properties" *Materials Science Forum*. Trans Tech Publications, Switzerland, v. 803, pp. 179-184, 2015.

[21] SCRIVENER, K. L.; CAPMAS, A. "Calcium aluminate cements". In: *Lea's Chemistry of Cement and Concrete*. Ed. Arnold, Londres. 1998:709-778.

[22] SILVA FILHO, S. H.; BIESEKI, L.; MAIA, A. A. B.; TREICHEL, H.; ANGELICA, R. S.; PERGHER, S. B. C. "Study on the NaOH/metakaolin ratio and crystallization time for zeolite a synthesis from kaolin using statistical design", Materials Research, v. 20, n. 3, pp. 761-767, 2017.

[23] Azevedo AGS, Streckera K, Barrosa LA, Tonholo LF, Lombardi CT. Effect of curing temperature, activator solution composition and particle size in brazilian fly-ash based geopolymer production. Materials Research, 2019;22(suppl.1): e20180842.